Fire performance of closed-cell charring insulation materials in plasterboard insulation assemblies

FIRE PERFORMANCE OF CLOSED-CELL CHARRING INSULATION MATERIALS IN PLASTERBOARD-INSULATION ASSEMBLIES

Juan P. Hidalgo*[1,2], José L. Torero[2], and Stephen Welch[1]
[1]School of Engineering, BRE Centre for Fire Safety Engineering, Institute for Infrastructure and Environment, The University of Edinburgh, Edinburgh, EH9 3FB, UK
[2]School of Civil Engineering, The University of Queensland, Brisbane, QLD 4072, Australia
[3]A. James Clark School of Engineering, University of Maryland, College Park, MD 20742, USA

Abstract

This paper presents an experimental study on the fire performance of two types of plastic charring insulation materials when covered by a plasterboard lining. The specific insulation materials correspond to rigid closed-cell plastic foams; a type of polyisocyanurate (foam A) and a type of phenolic foam (foam B), whose thermal decomposition and flammability were characterised in previous studies. The assemblies were instrumented with thermocouples. The plasterboard facing was subjected to constant levels of irradiation of 15, 25 and 65 $kW \cdot m^{-2}$ using the Heat-Transfer Rate Inducing System. These experiments serve as (1) an assessment of the fire behaviour of these materials studied at the assembly scale, and (2) an identification of the fire hazards that these systems pose in building construction. The manifestation of the hazards occurred via initial pyrolysis reactions and release of volatiles followed by various complex behaviours including char oxidation (smouldering), cracking and expansion of the foam. Gas-phase conditions may support ignition of the volatiles, sustained burning and ultimately spread of the flame through the unexposed insulation face. The results presented herein are used to validate the insulation 'critical temperature' concept used for a performance-based methodology focused on the selection of suitable thermal barriers for flammable insulation.

Keywords

Insulation materials; charring foams; pyrolysis; smouldering; plasterboard

1 Introduction

At present, insulation materials are being increasingly adopted in the built environment due to strict requirements on energy performance[1]. In the recent decades, energy efficiency has become one of the primary drivers in building construction aiming at a more sustainable world. These requirements are pushing towards building envelopes with significantly low thermal transmittance (*U-value*); thus, larger insulation thickness is needed in energy-efficient buildings. Given the multi-criteria nature of building design, this poses a challenge in relation to other design criteria such as space usage, change in construction techniques, and cost. Closed-cell plastic insulation materials, e.g. rigid polyisocyanurate and phenolic foams, are characterised by their relatively low thermal conductivity (0.02 – 0.03 $W \cdot m^{-1} \cdot K^{-1}$). Thus, they are often presented as a better solution against other common inorganic insulation materials, e.g. stone or glass wools (0.03 – 0.04 $W \cdot m^{-1} \cdot K^{-1}$). As a result, thinner walls, and therefore more efficient space usage, can generally be achieved more easily with plastic foams, if only energy efficiency is considered as governing design criterion. Nonetheless, the intense use of plastic foams in buildings introduces a series of fire hazards due to their combustible nature[2]. This is particularly relevant given the fact that fire safety is not normally considered as a quantifiable parameter in the multi-criteria building design problem, but purely as a prescriptive requirement based on material classification and pass-fail standard testing[3,4]. In order to adequately address the hazards posed by

combustible insulation in the design phase, a performance-based approach is necessary. The development of design tools for performance-based approaches requires a good understanding of the material behaviour so that the hazards can be identified and the risks diminished using mitigation measures.

1.1 Thermal degradation from charring closed-cell plastics

The first step towards a fundamental comprehension of the fire performance of materials is often made by characterising the thermal decomposition at the material and sample scale. Characterisation of the thermal decomposition experienced by several types of polyisocyanurate and phenolic foam insulation at high temperatures has been pursued by several authors[5,6,7,8,9,10,11]. Recently, Hidalgo *et al.*[12] presented thermogravimetric analyses (TGA) and an assessment of flammability parameters (critical heat flux for ignition and thermal inertia) through Cone Calorimeter testing[13] for the specific materials studied within their research framework. Further work was developed to study the pyrolysis and smouldering processes of these foams in relation to temperature measurements within the solid phase under constant levels of nominal irradiation[14]. The fire performance was found to be strongly determined by their closed-cell structure and charring behaviour, i.e. they present resistance to gas diffusion through the porous media and are characterised by leaving a carbonaceous residue (char) after pyrolysis. The former limits the smouldering behaviour, while the latter reduces the net heat flux delivered to the pyrolysis zone and, therefore, the release of flammable gases and resulting heat release rate.

Characteristic TGA results for the specific polyisocyanurate and phenolic foams studied herein with a heating rate of 10 °C·min^{-1} in different atmospheres (nitrogen, air, and the residue obtained in nitrogen exposed to air) are presented in Figure 1. In inert atmospheres, the polyisocyanurate foam (foam A) is shown to leave a residue of (22 ± 1) % from its original mass at 800°C, while the residue of the phenolic foam (foam B) is (45 ± 4) % (refer to the blue diamond series in Figure 1a/b). This indicates that overall, in non-oxidative conditions, a larger mass is pyrolysed from the foam A than the foam B; therefore, a larger release of flammable gases is to be expected for the foam A under these conditions. The temperature at which the main release of pyrolysis gases is obtained corresponds to approximately 275 – 350°C for foam A and 400 – 475°C for foam B. The residue from both foams obtained in the absence of oxygen (blue diamond series) proceeds to oxidise between 450 – 550°C when exposed to air (green triangle series in Figure 1). If the foam samples are directly exposed to air (refer to the red square series in Figure 1), the thermal degradation of foam A proceeds as two main well-differentiated reactions of a first pyrolysis and a posterior oxidation, while the main pyrolysis and oxidation reactions from foam B seem to overlap. The latter sequence of reactions is, however, not expected to occur in real end-use conditions, as the insulation is often covered by a lining or thermal barrier, and the presence of air at the surface of the foam is expected to be rather limited.

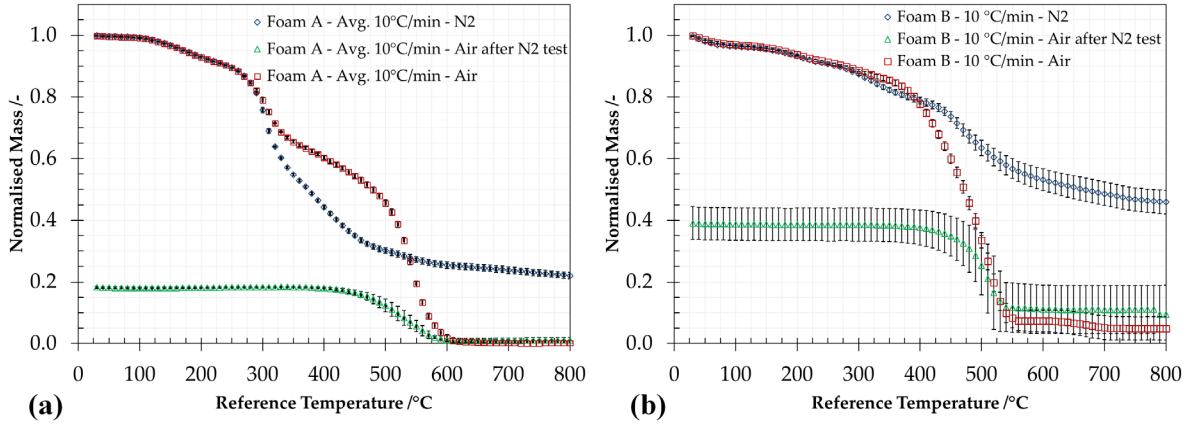

Figure 1. Thermogravimetric data from (a) foam A and (b) foam B materials in nitrogen and air, with a heating rate of 10 °C·min^{-1}. Error bars represent deviation from the average value for duplicates. Blue diamonds: test in nitrogen. Green triangles: Residue of test in nitrogen tested in air. Red squares: test in air.

Then, from a pyrolysis release (flaming) point of view, foam B apparently shows a less hazardous behaviour, with generally higher pyrolysis temperatures and larger char residue. However, in the presence of oxygen, foam B presents a worse behaviour as the pyrolysis and oxidation reactions are in the same temperature domain, as shown in the differential thermogravimetric (DTG) curves presented in Figure 2. This performance, which was further discussed elsewhere[14], indicates that the char from foam A is expected to play a more effective role than the char from foam B protecting the virgin material.

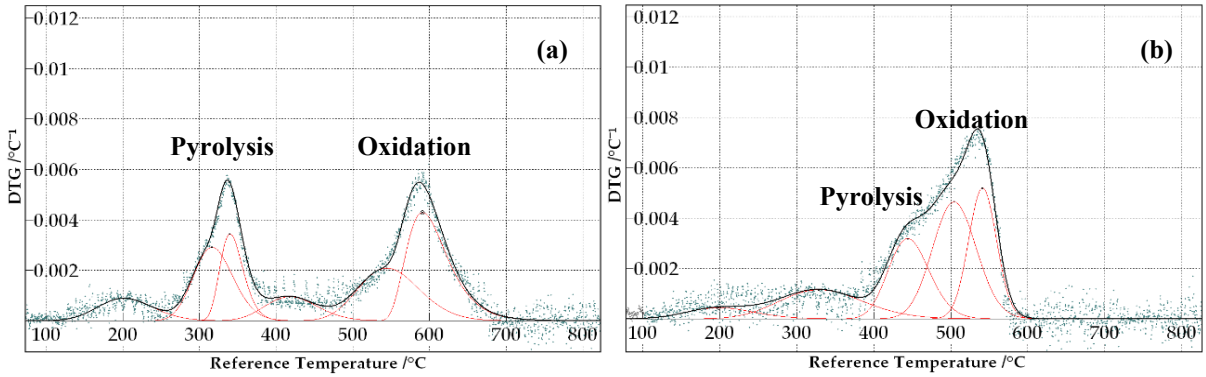

Figure 2. Differential thermogravimetric curves (DTG) for (a) foam A and (b) foam B obtained in air atmospheres under a heating rate of 20 °C·min^{-1}. A deconvolution technique[15] is used to identify the potential thermal degradation reactions using a Fraser-Suzuki regression[16,17] (red lines).

1.2 Performance-based methodologies for design of flammable insulation

A novel performance-based approach for the fire safe design of assemblies including insulation materials has recently been proposed[18]. This approach is based on the selection of suitable thermal barriers in order to control the onset of hazard, which for charring insulation materials is directly related to the release of flammable gases. This design philosophy is based on the control of the pyrolysis onset in order to guarantee that the insulation does not generate hazardous gases (flammable or toxic) under specific design fire scenarios. The concept of a 'critical temperature' from the insulation was proposed as a quantifiable variable to conservatively define the occurrence of this event[12]. Conservative values of critical temperatures for polyisocyanurate and phenolic materials were themselves conservatively selected as 300°C and 425°C, which are consistent with the thermogravimetric results presented in the previous section. The use of a thermal barrier, i.e. a thermally thick element inserted at the exposed face of the insulation, acts as thermal buffer delaying when the insulation surface achieves its critical temperature, which is proposed as the main failure criterion. Thus, this approach may serve to guarantee the fire safe use of combustible insulation for a certain period of time, which can be applied in RSET/ASET assessments for the fire safety strategy of the building[19].

The presented philosophy was defined on the basis of a hazards assessment for common insulation materials consisting of studies of the material behaviour at a small scale (thermogravimetric and Cone Calorimeter tests). Nevertheless, there is still need for verifying the interaction between insulation and lining, and further assessing the fundamental behaviour from the insulation at a larger scale. Additionally, reliable experimental data is needed to carry out validation studies for already proposed tools focussed on the design and selection of thermal barriers to control the onset of pyrolysis[20]. These tools compile the set of variables that define the heat transfer problem: insulation critical temperature, fire boundary condition, and barrier thickness and thermal properties.

1.3 Research objectives

An experimental programme is presented to explore the performance of two specific charring plastic insulation materials while subjected to different conditions of heat exposure, and used in conjunction with a common lining such as plasterboard in a controlled environment. The aims of this work are (1)

to present a verification of the fire hazards of these insulation materials presented in previous work[12,18]; (2) validate the concept of 'critical temperature' as the primary failure mode for flammable insulation materials to be used in buildings; (3) assess the evolution of the hazard represented by the rate of pyrolysates release; and (4) interrelate the fire behaviour of these materials at small and large sample scales.

To achieve the aforementioned objectives, this paper presents a thermal assessment of these assemblies and the use of a simplified method for estimating rates of pyrolysis from the insulation material when exposed to fire conditions[21,22]. The goal of this analysis is to support consistency between the 'critical temperature' concept and the consequently observed pyrolysis process experienced by the charring insulation material.

The quantitative outcomes from this study are limited to the two specific commercial polyisocyanurate and phenolic foams used within this research, defined as PIRb and PF in previous studies[12]. The general issues associated with sample identification and results generalisation have recently been highlighted in a letter regarding materials identification sent to fire journal editors[23]. Specifically, as discussed in related previous work[24], several formulations may be found for isocyanurate-based and phenolic-based foams, with a wide range of products offered by multiple manufacturers. Additionally, the formulation of these materials is generally confidential and not publicly accessible. Thus, the fire performance of the materials used for this research may not be representative of the whole generic material group. Extrapolation must be done with great care, and requires an explicit characterisation of the thermal decomposition and flammability of the specific material[12]. The work presented herein provides an expansion of the framework for the fire safe use of insulation materials. Application of this framework to specific products requires developing dedicated data sets.

2 Methodology

2.1 Materials

The types of charring insulation material studied were specifically a commercial rigid closed-cell polyisocyanurate foam and a commercial rigid closed-cell phenolic foam, identical to the materials characterised in previous studies[12,14]. Noting the concerns regarding a potential inadequate extrapolation of the fire performance of these specific products to the performance of generic material groups[23], the polyisocyanurate and phenolic foam used within this work are hereafter denoted as foams A and B, respectively. The insulation materials were supplied as rigid boards with a foil-facing on the surface. Whereas in previous research the foil was removed to study the performance of the insulation in isolation, the insulation boards were not modified for this work. The measured density of insulation foams A and B was approximately 33.0 $kg \cdot m^{-3}$ and 38.1 $kg \cdot m^{-3}$, respectively. A 12.5 mm thick commercial brand of fire-rated plasterboard was used, rated as type A and F according to BS EN 520[25]. The commercial density of the plasterboard was 10 $kg.m^{-2}$.

2.2 Experimental: instrumentation and testing method

The size of the insulation board samples was cut to an approximate size of 450 mm (wide) by 760 mm (tall), and 100 mm (thick). The insulation was placed within a steel frame with the same internal dimensions, so that the insulation fitted tightly into the frame. The system frame-insulation was covered by a plasterboard leaf of dimensions 600 mm by 800 mm, thus the insulation and frame remained covered during the experiments. The plasterboard was fixed onto the frame with clamps. This system allowed free expansion or contraction of the plasterboard, since the aim of this work was to explore the behaviour of the insulation relying on the non-failure (integrity) of the lining.

A representation of the sample holder and set-up is shown in Figure 3a and Figure 4. The test samples consisting of the plasterboard leaf and the insulation board were exposed to a radiative heat source. The system used was H-TRIS (Heat-Transfer Rate Inducing System)[26], which allows moving the radiant panels onto different positions in order to represent a different level of irradiation on the surface of the

sample being tested. The calibration process to define the relation between heat flux and panels-sample distance is done with a water-cooled Schmidt-Boelter gauge, as shown in Figure 3b. The nominal irradiation exposures for these tests were 15, 25, and 65 $kW \cdot m^{-2}$.

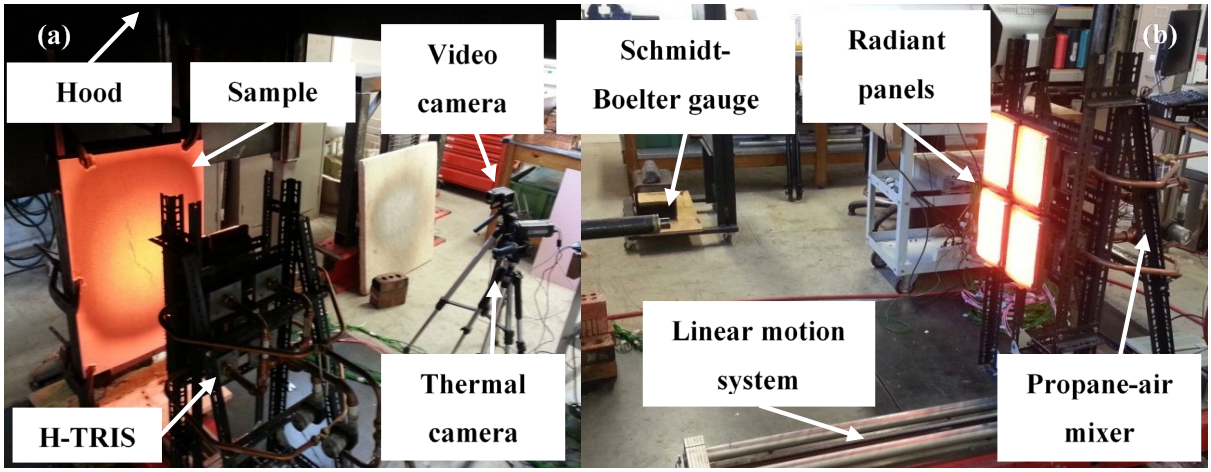

Figure 3. (a) Experimental set-up with sample, sample holder, H-TRIS, and instrumentation. (b) H-TRIS system during calibration using a Schmidt-Boelter gauge.

Each insulation sample was instrumented with several 1.5 mm K-type thermocouples. As shown in Figure 4b/c, the thermocouples were inserted in the core of the insulation material at three different positions and different depths, and perpendicular to the exposed surface. The thermocouples were positioned at the plasterboard rear surface, and every 20 mm in-depth from that position up to the back surface of the insulation. No thermocouples were inserted within the plasterboard so as not to damage the lining nor induce any initial cracking. Instead, an FLIR® A320 thermal camera was used to estimate the surface temperature of the plasterboard (Figure 3a). An emissivity of 0.9 ± 0.1 for the plasterboard[27,28,29] was used to account for the uncertainty in the surface temperature measurement with the thermal camera.

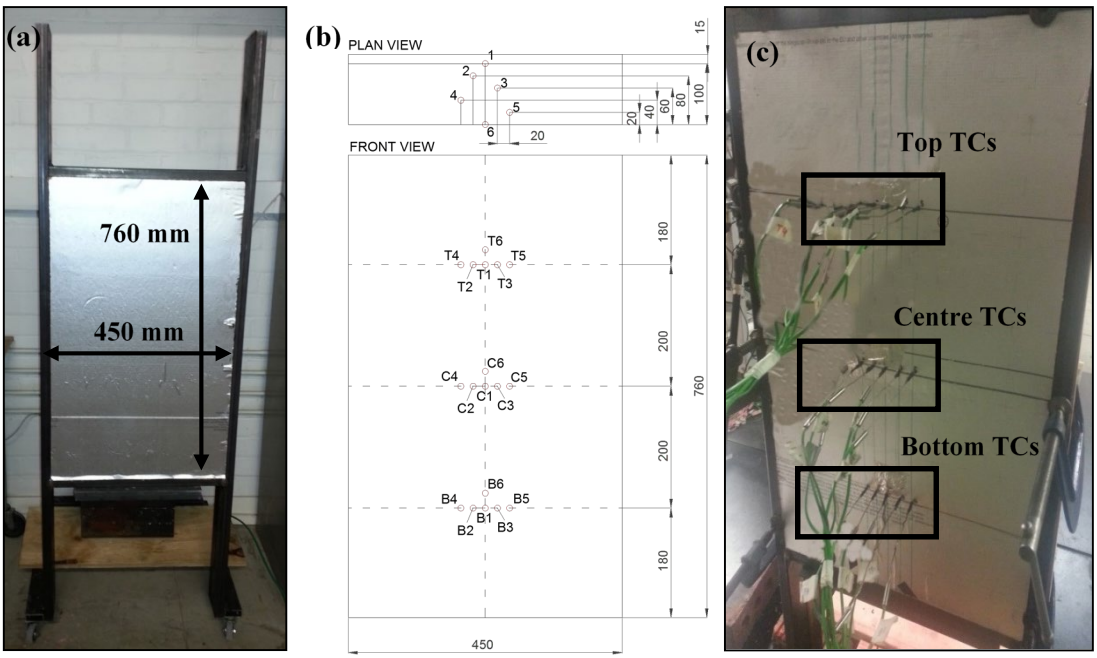

Figure 4. (a) Steel frame with embedded insulation board prior to attaching the plasterboard lining. (b) Schematics of thermocouple positioning. (c) In-depth thermocouples configuration.

2.3 Analysis methodology

To assess the fire hazards related to the use of flammable insulation such closed-cell charring foams A and B in an assembly of this type, it is necessary to evaluate the pyrolysis onset at the surface of the insulation and posterior flaming or smouldering combustion processes. The use of thermocouples is essential to determine the instant at which the insulation starts pyrolysing ('critical temperature'), and therefore establish a conservative primary failure mode consistent with previous work[12,18]. Given that the plasterboard is placed at the surface of the insulation, it is expected that pyrolysis gases may not be able to establish a flame at this surface, but be released by cracks or gaps from the assembly.

Determining the pyrolysates rate released from the insulation is essential to assessing the evolution of the hazard. A simplified method proposed by Hidalgo *et al.*[21,22] to obtain pyrolysis rates from charring materials based on temperature measurements is applied to the measured temperature obtained in this experimental programme. The approach consists in assuming that the sample is divided into finite differences with a bulk temperature obtained by interpolation from the thermocouples' readings. The mass of each finite difference during the test is obtained as a function of the TGA data in non-oxidative conditions with a constant heating rate. This approach was successfully applied for 100 mm thick samples of foam A with a 3 mm thick metallic plate tested with the Cone Calorimeter, and using TGA data with 2.5 and 20 °C·min^{-1} heating rates[22]. Different heating rates are used to define an uncertainty region because, although low heating rates are expected for these materials, the heating rate at the pyrolysis region is not necessary evolving at a constant speed. Although a perfect fitting between model and experiments was not achieved using this method due to the number of applied simplifications, the results provided a reasonably good prediction of the pyrolysis process from foam A[22]. Given the similarity of conditions in the thermal evolution obtained for this series of experiments, i.e. use of a thermal barrier on the surface of the insulation, this method is expected to provide an adequate indication of the pyrolysis process.

In order to address the effectiveness of the thermal barrier used for this set of experiments, the aforementioned analysis methods are applied: (1) identification of the time to reach the pyrolysis onset ('critical temperature') on the surface of the insulation, and (2) identification of the estimated pyrolysis rate experienced by the insulation.

3 Results

3.1 Thermal evolution and highlighted events for the 'plasterboard – foam A' assembly

The time-history of temperatures for 'plasterboard – foam A' assemblies under external heat fluxes of 15, 25 and 65 kW·m^{-2} is shown in Figure 5. These temperature measurements correspond to the centre position, as it represents the region where more uniformity in the external heat flux is obtained. The temperature range indicating the main pyrolysis domain for foam A is included in the charts as a horizontal shading region between 300°C and 350°C. A series of patterns can be observed in these temperature profiles:

- The surface temperature of the plasterboard does not evolve as would be expected from an inert behaviour, with a change in the curvature as shown in Figure 5a/b, where an inert dotted baseline is projected. The observed increase in the surface temperature is due to (1) the oxidation of the back-face render of the plasterboard and (2) the flaming at the surface of the plasterboard from pyrolysis gases escaping through cracks in the plasterboard.
- A peak on the surface temperature is observed for the experiment at 65 kW·m^{-2} after one to two minutes of the test (Figure 5c), with a peak temperature in the range 650 – 750°C. These results are consistent with the visual observations that verified the oxidation of the front face render (paper) of the plasterboard.
- A plateau of temperatures around 100°C is observed for the thermocouple at the interface between the plasterboard and the insulation board, indicating a significant endothermic process taking place within the plasterboard during the heating. This plateau, likely due to vaporisation

of moisture within the plasterboard, is consistently shorter for larger external heat fluxes.

Figure 5a shows a case study where the surface of the insulation board marginally achieves the critical temperature of 300°C for foam A. Indeed, the plasterboard surface achieves a temperature of approximately 330°C during the steady-state. An irregularity is observed at the interface thermocouple (C1) at 15 min, indicating a bad positioning of the thermocouple which was later corrected. Some small cracks were observed on the surface of the plasterboard after 70 min of the test, as well as some expansion of the insulation board after 72 min, which seemed to push the plasterboard out. Some vapours were observed after 75 min of the test, coinciding with the time when the interface reached temperatures near the critical temperature. However, it was visually assessed that the release of volatiles was minor.

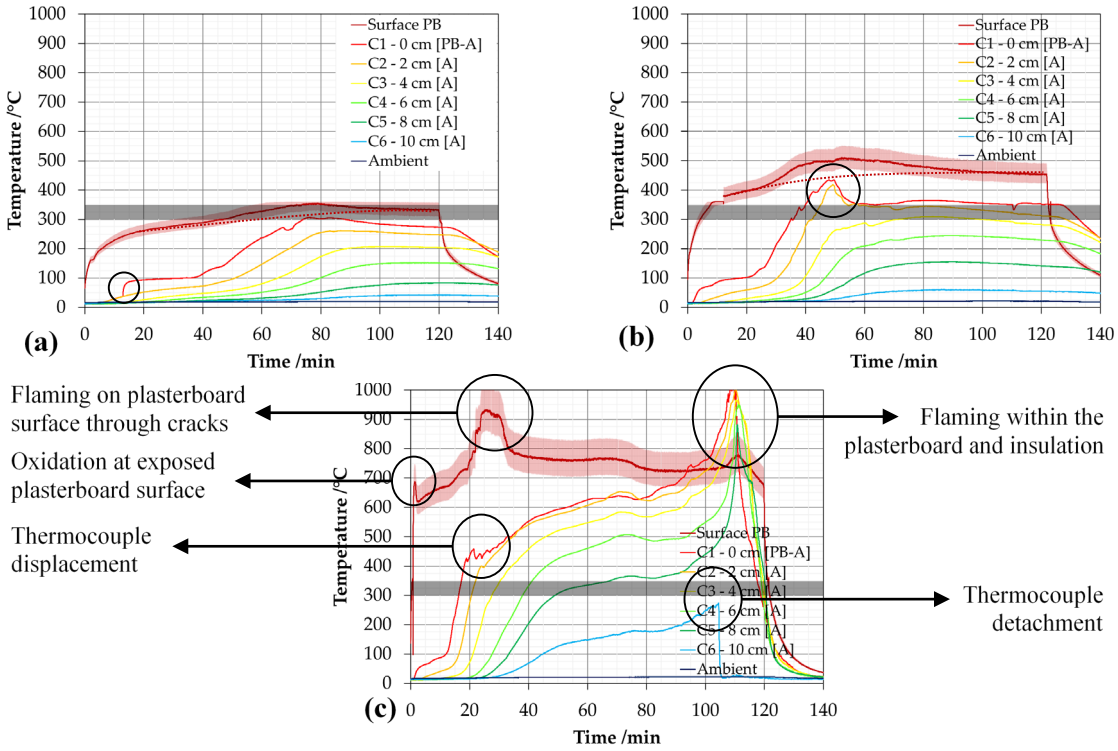

Figure 5. Time-history of temperatures within the 'plasterboard – foam A' assembly tested under external heat fluxes of (a) 15, (b) 25, and (c) 65 kW·m^{-2}. Shading in the surface temperature indicates the sensitivity of its quantification in relation to an emissivity within ε = 0.9 ± 0.1. Horizontal shading represents the presumed/nominal pyrolysis domain.

Figure 5b shows a case study where the surface of the insulation board achieves the critical temperature after 35 min of the test. Consistently, the release of vapours from the edges of the plasterboard was observed from 36 min to approximately 50 min. Some cracks were observed in the plasterboard with the release of grey-black smoke, leaving a pattern of soot deposition on the plasterboard surface. Additionally, the sample was found to expand 10 mm at the centre from the back of the frame, which was identified by the significant movement of the interface and C2 thermocouples, observed at 49 min. Eventually, as noted in Figure 5b, a thermal equilibrium was obtained from 60 min.

Figure 5c shows a case study where surface oxidation consumed the plasterboard's exterior render after 1 min of the test. A significant amount of vapours, probably mainly moisture, were released from the plasterboard during the first 5 min of the test. The release of volatiles through the plasterboard-frame edges was observed after 17 min, which is consistent with the interface achieving the critical temperature of 300°C at 16 min. After 20 min, flaming was observed from the cracks of the plasterboard surface, which was verified by the significant increase of surface temperature (above 900°C) recorded by the thermal camera between 21 and 33 min. The thermocouple measurement at the interface shows a drop just after 20 min, suggesting the expansion of the insulation board, which is confirmed by the 40 mm movement of the back face of the board from its original position, and the gap between the

plasterboard and the surface of the insulation. An approximately steady state is observed in the temperatures between 40 and 80 min, at which point a sudden temperature increase is observed for all the thermocouples in the core of the insulation. Dark smoke was observed, suggesting that this enhanced temperature increase was due to smouldering of the char within the frame. After 95 min, flaming was observed between the edge of the insulation and the top of the frame. The flames finally broke through the insulation board, and flaming was observed at the back face of the board and top, as shown in Figure 6. These events are represented by the accelerated increase of temperature shown in Figure 5c from 100 min until 110 min. Large pieces of char remained from the board, and they continued to glow (smoulder) after the end of the experiments.

Figure 6. Evolution of the back face of the foam A board tested at 65 kW·m^{-2} at 100-110 min, with smouldering/flaming breaking through.

3.2 Thermal evolution and events for the 'plasterboard – foam B' assembly

The time-history of temperatures for 'plasterboard – foam B' assemblies under external heat fluxes of 15, 25 and 65 kW·m^{-2} are presented in Figure 7. Most of the events observed from foam A samples, for instance, the oxidation of the exterior and interior render of the plasterboard, and the plateau of temperatures at 100°C, were also observed for these cases. The critical temperature proposed in previous work[12] of 425°C for foam B is indicated as a horizontal shading region from 400°C to 450°C.

Figure 7a shows the time-history of temperatures of a case study where the insulation board does not achieve the critical temperature (15 kW·m^{-2}), since the plasterboard surface and plasterboard-insulation interface achieve a maximum temperature of only 350°C and 386°C, respectively. The temperature profile within the insulation board achieves an approximately steady state after 80 min, but including a minor continuing increase in temperature, likely due to oxidation reactions at the interface. This oxidation is likely related to the back face render of the plasterboard, as shown previously. However, its longer duration suggests oxidation at the surface of the insulation as well. After the heating is removed, the temperatures continue to drop, indicating that if smouldering combustion had been produced at the surface of the insulation, this did not progress any further. No apparent release of vapours was observed during the experiment, but spalling sounds were recorded from 55 min until the end of the test when the temperature at the interface is 190°C and the thermocouple C1 records 110°C. Additionally, a plateau of temperatures at approximately 100°C is observed.

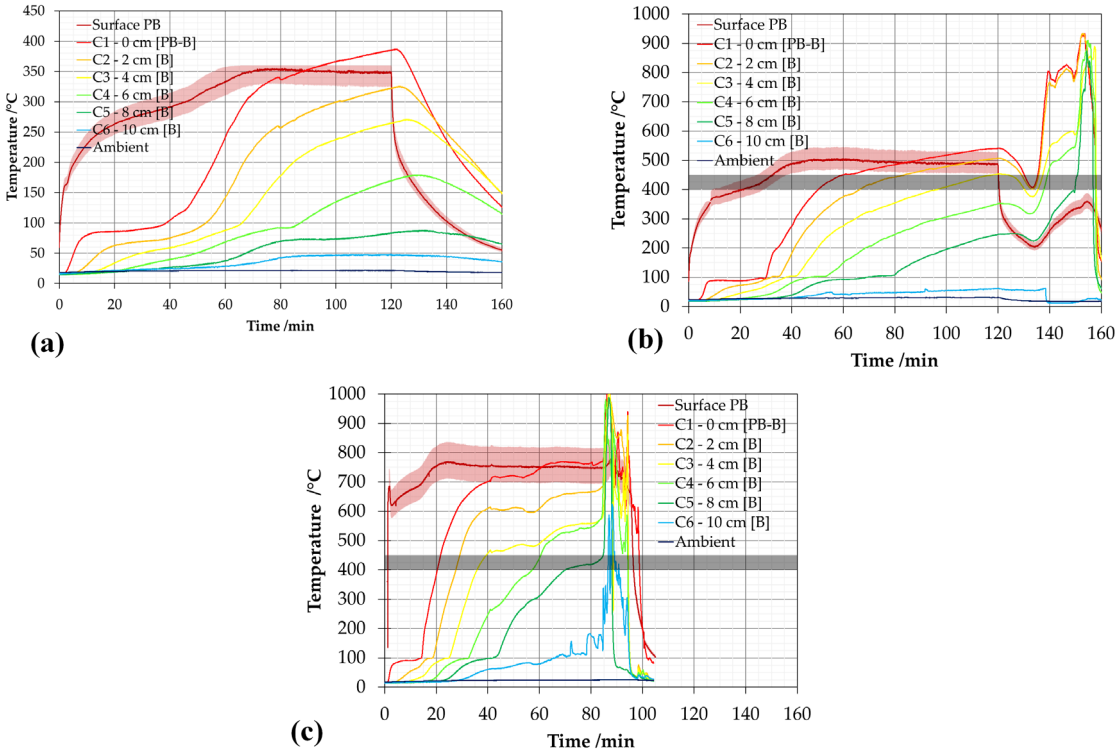

Figure 7. Time-history of temperatures within the 'plasterboard – foam B' assembly tested under external heat fluxes of (a) 15, (b) 25, and (c) 65 kW·m^{-2}. Shading in the surface temperature indicates the sensitivity of its quantification in relation to an emissivity within ε = 0.9 ± 0.1.

Figure 7b shows the time-history of temperatures of a case study where the critical temperatures is attained. Indeed, the interface reaches a temperature of 425°C at 54 min after the initiation of the test. Similarly to the previous case, spalling sounds were heard from 25 min until the end of the test. The temperature plateau at 100°C is also identified for the interface. Additionally, positions C2 to C5 experience a clear plateau also around 100°C, likely corresponding to water desorption from the polymer. Thermocouples C2 (20 mm) and C3 (40 mm) are found to cross the critical temperature at 73 min and 106 min, respectively, which suggests the release of pyrolysates. The temperature at the interface achieves an approximately steady state from 60 min, but slowly increases to a rate of about 1.7 °C·min^{-1}, which is also observed for the temperatures in the core of the insulation. This heating occurs via smouldering combustion at the surface of the insulation board (interface), which was confirmed by the release of minor amounts of smoke through the plasterboard cracks formed at the front. After the radiant panels were turned off at 120 min, the temperatures initially drop, but at 130 min the temperatures start to increase again without the presence of an external heat source. Visual observations indicate flaming behind the plasterboard at 130 min. Eventually, flaming broke through the insulation and spread on the back face of the insulation. This is represented by the significant temperature increase observed between 130 and 160 minutes in Figure 7b. It is thought that this behaviour resulted from the radiant panels being turned off, which had helped to cool down the assembly, and therefore caused the pressure to drop and the plasterboard to contract, allowing higher diffusion of air into the assembly. As a result, the char from the foam B was at sufficient temperatures to oxidise.

Figure 7c shows a case study under a heat exposure of 65 kW·m^{-2}. The critical temperature is achieved at the interface after 21 min, while thermocouples C2 (20 mm), C3 (40 mm), C4 (60 mm) and C5 (80 mm) reach this temperature after 28, 37, 59 and 82 min, respectively. This qualitatively indicates an increased release of pyrolysates, which was confirmed by flaming at the surface of the plasterboard from the cracks formed, shown in Figure 7c when the surface reaches 900°C. Unlike the experiment at 25 kW·m^{-2}, the flames break through the insulation board before the radiant heaters are turned off. As a result, fire spreads at the back surface of the insulation board as shown in Figure 11b below, finally consuming all the insulation, while the remaining pieces of char were consumed by smouldering.

3.3 Fraction of thermal degradation and pyrolysis rates

The estimated mass per unit area and mass loss rate per unit area (pyrolysis rate) of the sample for the foam A experiments are presented in Figure 8. It should be noted that since the density of foam A was calculated as 33.0 kg·m^{-3}, and the thickness of the insulation board was 100 mm, the initial mass per unit area of the insulation board is 3.30 kg·m^{-2}. Additionally, the curves are calculated without considering the oxidation of the char, which is why Figure 8c shows some mass loss remaining after 100 min. Figure 8a confirms that no significant pyrolysates are released during the experiment at 15 kW·m^{-2} (Figure 5a). The minor release of volatiles is calculated between 60 and 80 min of the test, with a maximum of 0.1 g·m^{-2}·s^{-1} around 74 – 75 min, which is in agreement with the visual observations that indicated a minor release of volatiles from the insulation. Figure 8b shows that the release of pyrolysates for the test at 25 kW·m^{-2} (Fig. 3b) is observed from 30 to 50 min, with a maximum rate of 0.8 – 1 g·m^{-2}·s^{-1} from 40 to 47 min. Figure 8c (65 kW·m^{-2}) shows a more severe reaction behaviour, with pyrolysates released from 15 min, and achieving a maximum of 1.3 g·m^{-2}·s^{-1} approximately at 21 min. The rate of mass loss decreases until being null at 80 min, after which the rate continues to increase again up to 0.4 g·m^{-2}·s^{-1}. This increase is explained by the temperature growth in the insulation core due to smouldering combustion with renewed oxygen, thus displacing the pyrolysis front into the remaining virgin material.

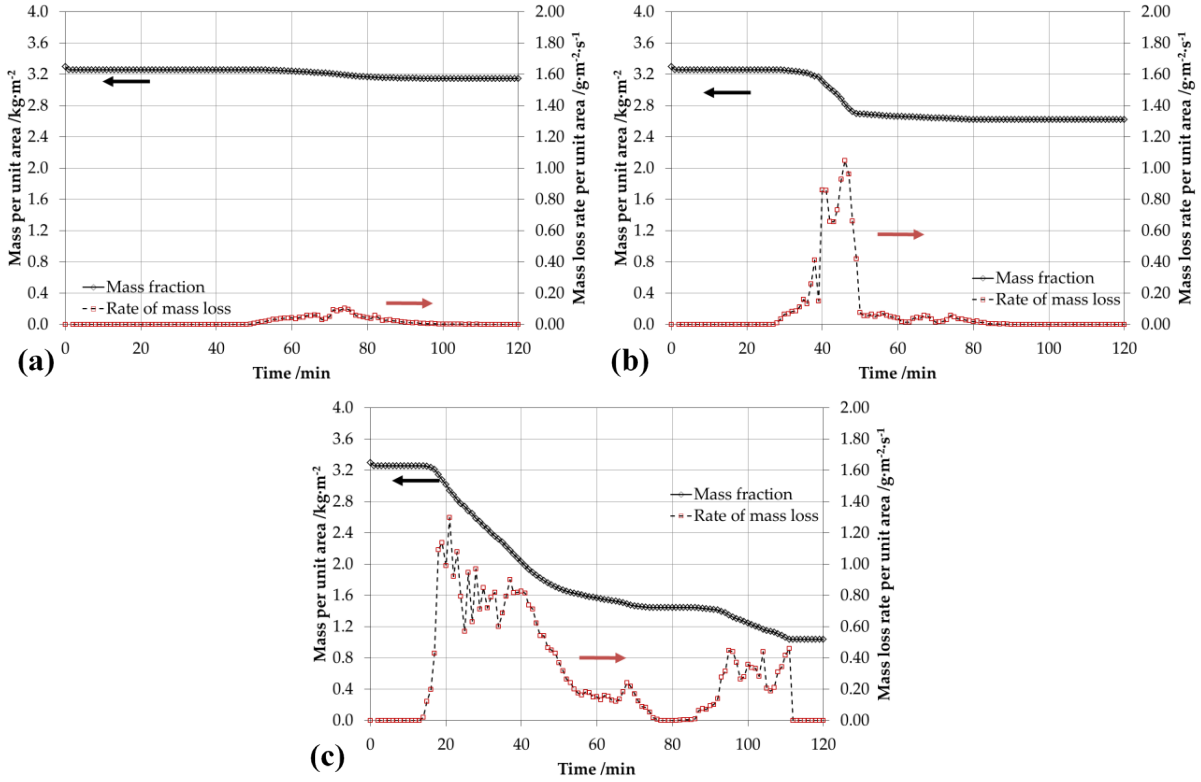

Figure 8. Estimated mass per unit area (solid line) and pyrolysis rate (dashed line) of foam A for assemblies tested under external heat fluxes of (a) 15 kW·m^{-2}, (b) 25 kW·m^{-2} and (c) 65 kW·m^{-2}.

The temporal evolution of the fraction of remaining mass from the experiments at 15 kW·m^{-2} and 25 kW·m^{-2} is presented in Figure 9, together with sections from the core of the insulation samples, which indicates the degree of thermal degradation by the insulation discolouration. The section of the sample tested at 15 kW·m^{-2} shows significant cracking and a related thickness expansion of up to 10 mm, while the section tested at 25 kW·m^{-2} presents more severe cracks and a final total thickness of approximately 120 mm.

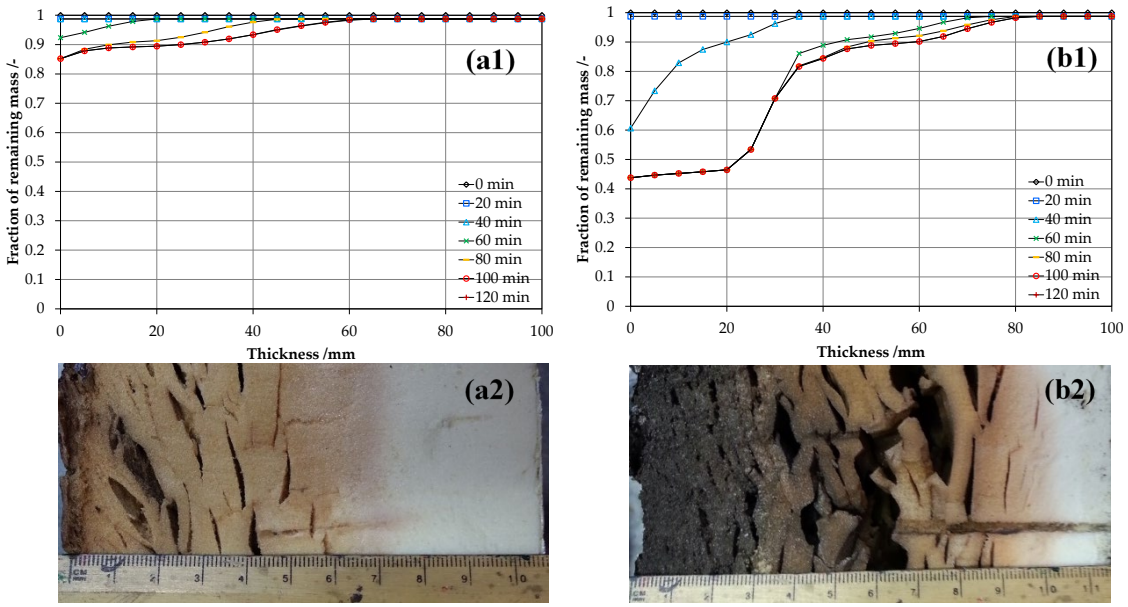

Figure 9. Estimated fraction of remaining mass of foam A under external heat fluxes of (a1) 15 kW·m^{-2} and (b1) 65 kW·m^{-2} and their residue at the end of the test (a2 and b2).

The estimated mass per unit area and mass loss rate per unit area (pyrolysis rate) of the sample for the foam B experiments are presented in Figure 10. It should be noted that since the density of foam B was found to be 38.1 kg·m^{-3} and the thickness of the insulation board was 100 mm, the virgin mass per unit area of the insulation board is 3.81 kg·m^{-2}. Figure 10a/b indicate that the maximum release of pyrolysates was moderate at 15 and 25 kW·m^{-2}, achieving a maximum of 0.10 and 0.20 g·m^{-2}·s^{-1} at 67 and 46 min, respectively. Figure 10c shows a maximum between 1.3 and 1.4 g·m^{-2}·s^{-1} between 29 and 39 min. The times when pyrolysis gases were released are consistent with the visual observations noted in the previous section.

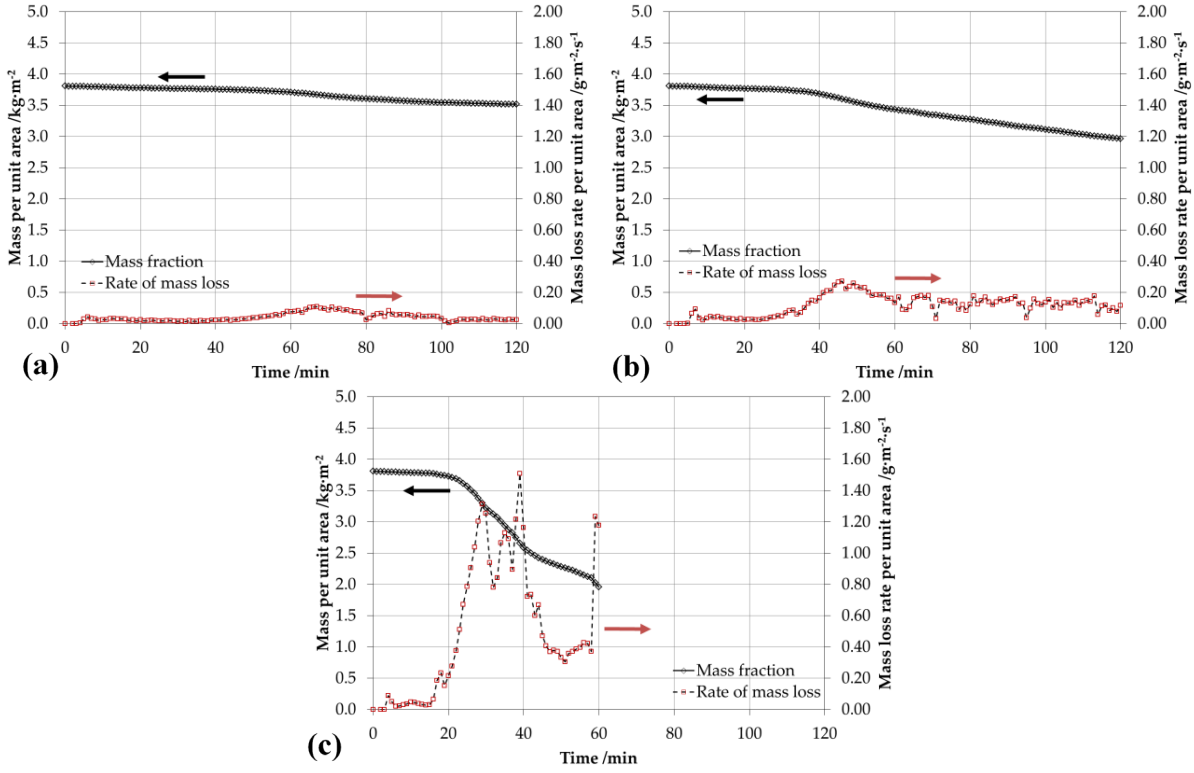

Figure 10. Estimated mass per unit area (solid line) and pyrolysis rate (dashed line) of foam B for assemblies tested under external heat fluxes of (a) 15, (b) 25, and (c) 65 kW·m^{-2}.

The temporal evolution of the fraction of remaining mass from the experiment at 15 kW·m^{-2} is presented in Figure 11, together with a section from the core of the insulation sample, which indicates the degree of thermal degradation by the insulation discolouration. The section of the sample shows limited cracking and no significant thickness expansion. Figure 11b illustrates the combustion on the back face for the 65 kW·m^{-2} test after 80 min.

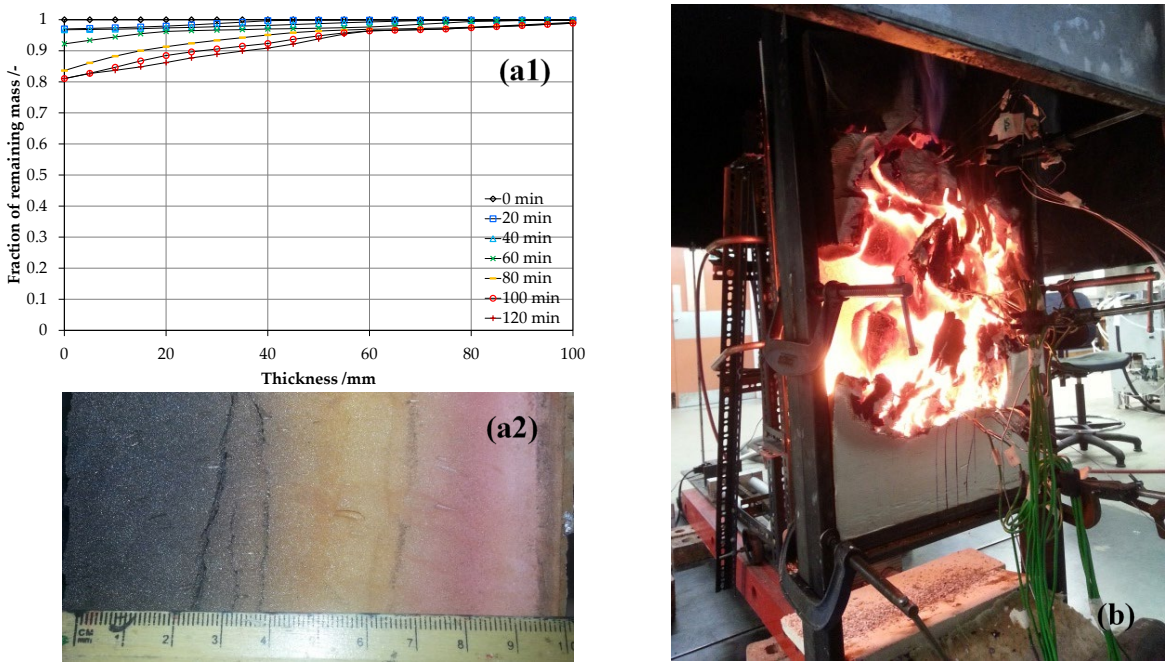

Figure 11. Estimated fraction of remaining mass of foam B under external heat flux of 15 kW·m^{-2} and the residue at the end of the test (a1 and a2), and combustion of foam B from the back face at 65 kW·m^{-2} after 80 min (b).

4 Discussion

4.1 Comparative performance of foams A and B

As highlighted previously, the critical temperature for foam A (300°C) is significantly lower than for foam B (425°C). While this difference may appear not significant, especially if the insulation is directly exposed to the fire, this work has demonstrated the different performance of both foams when protected by a thermal barrier. As shown in Table 1, the 'plasterboard-foam B' assembly takes a significantly longer time to reach the critical temperature than the 'plasterboard-foam A' assembly; 55% and 24% longer for 25 kW.m^{-2} and 65 kW.m^{-2}, respectively, while for 15 kW.m^{-2} the critical temperature is not achieved for foam B but it is reached for foam A.

In terms of the pyrolysis rate (MLR), it is shown that foam A achieves a larger value than foam B when tested at 25 kW.m^{-2}, which is consistent with the foam A pyrolysis temperature occurring at lower values compared to foam B (refer to Figure 2). However, at 65 kW.m^{-2}, the MLR for foam B is slightly larger than for foam A. These results are indicative of the pyrolysis and oxidation reactions for foam B occurring in broadly the same temperature domain, thus the char being less effective as shown in bench-scale experiments from previous work[14].

Table 1. Time to reach the critical temperature and estimated maximum mass loss rate per unit area for different assemblies under 12, 25 and 65 kW.m^{-2}.

Sample \ Heat flux	15 kW.m^{-2}	25 kW.m^{-2}	65 kW.m^{-2}
Plasterboard-foam A	t_{cr} = 75 min	t_{cr} = 35 min	t_{cr} = 16 min

	MLR_{max} = 0.1 g·m^{-2}·s^{-1} (75 min)	MLR_{max} =1 g·m^{-2}·s^{-1} (46 min)	MLR_{max} =1.3 g·m^{-2}·s^{-1} (21 min)
Plasterboard-foam B	t_{cr} not achieved MLR_{max} = 0.1 g·m^{-2}·s^{-1} (67 min)	t_{cr} = 54 min MLR_{max} = 0.3 g·m^{-2}·s^{-1} (46 min)	t_{cr} = 21 min MLR_{max} = 1.5 g·m^{-2}·s^{-1} (39 min)

4.2 Effectiveness of the thermal barrier

As previously introduced, the safe use of flammable insulation materials relies on the nature of the thermal barrier placed on the surface of the insulation; the thermal properties and thickness of the barrier are critical to controlling the characteristic time of the pyrolysis onset. Therefore, the selection of suitable thermal barriers is essential to enable the use of these materials. In order to discuss the effectiveness of the thermal barrier, the MLR experienced by the foam A insulation studied herein is explored when different surface protections are used (refer to Figure 12). The three cases studied correspond to an exposure of 65 kW.m^{-2} for (1) an exposed foam A sample tested with the Cone Calorimeter[12] (no protection); (2) a foam A sample with a 6 mm Monel 400 plate on the surface tested with the Cone Calorimeter[Error! Bookmark not defined.]; and (3) a foam A board with a plasterboard on the surface (refer to Figure 8).

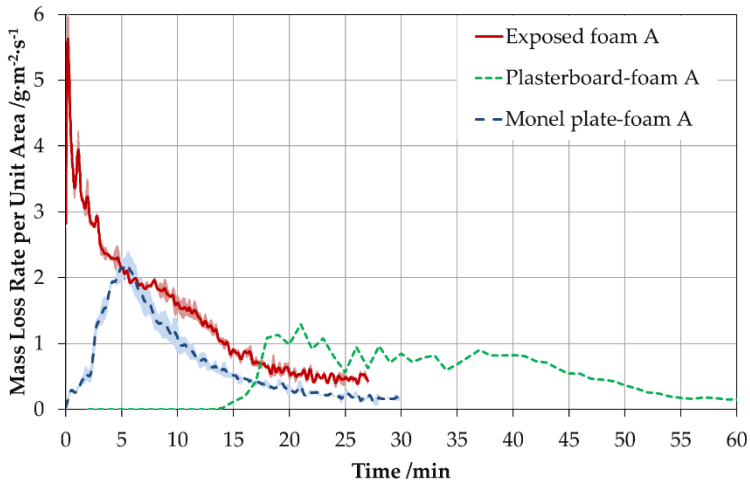

Figure 12. Mass loss rate per unit area for exposed foam A (red solid line)[12], a monel plate-foam A sample (blue dashed line)[22] and plasterboard-foam A (green dashed line) from the present work when exposed to 65 kW.m^{-2}.

Figure 12 shows that when exposed, the foam proceeds to pyrolyse instantly after the heat exposure onset, which is as expected, due to the low thermal inertia of the material. When protected by a thermally thin element of significant thermal mass (6 mm Monel 400 plate), the pyrolysis onset is not significantly reduced; however, the time to reach a peak MLR is delayed. For the case studied herein (plasterboard – foam A), the effect the plasterboard has on delaying the pyrolysis onset is clear, amounting to approximately 15 min from the heat exposure onset.

Another interesting aspect to consider is the reduction in MLR experienced by different protections. It is expected that if the protection is a thermally thin element of low thermal mass, the time to reach a peak MLR would be much faster as shown by Hidalgo *et al.*[18] and Crewe *et al*[30]. In the case of a thermally thick protection such as the plasterboard, it is clearly shown that the peak MLR is below the limit of 2 g.m^{-2}.s^{-1}. At this rate, it is unlikely that self-sustained burning would occur; however, flaming may be achieved under particular conditions as observed in these experiments.

5 Conclusions

This paper presents a series of experiments that have as objective to characterise the fire hazards that charring closed-cell insulation materials pose in building construction, thus expanding on the performance-based framework for the fire safe use of insulation materials. For that purpose, two specific commercial insulation materials characterised in previous studies[12,14], a rigid closed-cell polyisocyanurate foam (foam A) and a rigid closed-cell phenolic foam (foam B), have been used. The onset of hazard is defined here as the initial release of pyrolysis gases with other variables such as further oxidation of the char serving to modulate the potential consequences. Spread of the flame to the unexposed face of the insulation was given particular attention.

It has been observed that the release of pyrolysates from foams A and B is obtained after the interface lining-insulation reaches a critical temperature identified in previous work[12]. However, it is observed that the design methodology based on the critical temperature concept is conservative. For conditions of heat exposure that result in a thermal equilibrium with an interface temperature slightly above the critical temperature, minor rates of pyrolysis were obtained, which could not allow a flammable mixture. In contrast, for cases which generated slightly larger rates of pyrolysis (> 2 g.m^{-2}.s^{-1}), ignition could be achieved in many different ways, all of them difficult to characterise. This shows the intricacy of the problem after the onset of pyrolysis has been attained. Flaming conditions of the pyrolysis gas stream are strongly dependent on the mixing conditions, i.e. concentration of the flammable gases in the air, and the temperature of the mixture[31,32]. Establishing these conditions for building design is, therefore, very complex and not feasible with the context of construction processes. Therefore, the robustness of the approach based on a critical temperature seems to be justified overall, yet may be conservative for some particular scenarios. Additionally, a design philosophy based on the control of the onset of pyrolysis would aid mitigation of other fire risks due to the delay of other related hazards.

The simplified approach to determine pyrolysis rates has been shown to successfully represent the pyrolysis process at end-use scale, with the insulation covered by a common lining used in building construction. Given the charring nature of these foams and the constant values of irradiation used as external heat exposure, the pyrolysis rate patterns show a characteristic increase, maximum rate, and posterior decay. Nonetheless, if flaming at the plasterboard surface or further oxidation at the insulation are achieved, thus increasing the heat flux conducted to the insulation, the pyrolysis front suffers further displacement and further generation of flammable volatiles. Under real conditions, it would be expected that the pyrolysates released inside the compartment could accumulate and ignite, therefore generating a higher heat release rate and, consequently, a higher heat flux to the surface of the lining.

The use of a thermally thick barrier, such as a 12.5 mm thick plasterboard, is demonstrated to be effective in delaying the generation of pyrolysis gases from the plastic insulation, which otherwise would be almost immediately achieved if directly exposed[33]. However, the effectiveness of the thermal barrier is obviously dependent on parameters such as the external heat flux and the insulation critical temperature or any form of mechanical failure.

Further work is required to validate the already proposed tools for the selection of thermal barriers[20], and establish guidelines on the selection of common thermal barriers and their effectiveness as a function of thickness, design fire scenarios, and the insulation material adopted. The presented experiments represent a valuable set of data to expand the validation on a material such as plasterboard, and set the baseline for further thermal barrier validations. The methodology presented herein could contribute to reducing or mitigating the risks posed by combustible insulation in buildings.

6 References

[1] EU (2010). Directive 2010/31/EU of the European Parliament and of the Council of 19 May 2010 on the energy performance of buildings, *Official Journal of the European Union*, pp. 13-35. https://doi.org/10.3000/17252555.L_2010.153.eng

[2] Meacham, B., Poole, B., Echeverria, J., and Cheng, R., (2012). *Fire Safety Challenges of Green Buildings*. New York: Springer-Verlag. https://doi.org/10.1007/978-1-4614-8142-3

[3] British Standards Institution (2009). *BS EN 13501-1. Fire classification of construction products and building elements. Part 1: Classification using data from reaction to fire tests*.

[4] British Standards Institution (2012). *BS EN 1363-1. Fire resistance tests - Part 1: General Requirements*.

[5] Paul, K.T. (1984) Characterization of the burning behaviour of polymeric materials. *Fire and Materials*, 8(3), pp. 137-147. https://doi.org/10.1002/fam.810080304

[6] Buist, J.M., Grayson, S.J., and Woolley, W.D. (1986). *Fire and Cellular Polymers*. Springer Netherlands. https://doi.org/10.1007/978-94-009-3443-6

[7] Cleary, T.G., and Quintiere, J.G. (1991). *Flammability Characterization of Foam Plastics (NISTIR 4664)*. [online] NIST. Available at: http://www.nist.gov/customcf/get_pdf.cfm?pub_id=912213 [Accessed 1 May 2016].

[8] Dick, C., Dominguez-Rosado, E., Eling, B., Liggat, J.J., Lindsay, C.I., Martin, S.C., Mohammed, M.H., Seely, G., and Snape, C.E. (2001). The flammability of urethane-modified polyisocyanurates and its relationship to thermal degradation chemistry. *Polymer*, 42(3), pp. 913-923. https://doi.org/10.1016/s0032-3861(00)00470-5

[9] Modesti, M., Lorenzetti, A., Simioni, F., and Checchin, M. (2001). Influence of different flame retardants on fire behaviour of modified PIR/PUR polymers. *Polymer Degradation and Stability*, 74(3), pp. 475-479. https://doi.org/10.1016/S0141-3910(01)00171-9

[10] Dominguez-Rosado, E., Liggat, J.J., Snape, C.E., Eling, B., and Pitchel, J. (2002). Thermal degradation of urethane modified polyisocianurate foams based on aliphatic and aromatic polyester polyol. *Polymer Degradation and Stability*, 78(1), pp. 1-5. https://doi.org/10.1016/S0141-3910(02)00086-1

[11] Auad, M.L., Zhao, L., Shen, H., Nutt, S.R., and Sorathia, U. (2007). Flammability properties and mechanical performance of epoxy modified phenolic foams. *Journal of Applied Polymer Science*, 104(3), pp. 1399-1407. https://doi.org/10.1002/app.24405

[12] Hidalgo, J.P., Torero, J.L, and Welch, S. (2016). Experimental Characterisation of the Fire Behaviour of Thermal Insulation Materials for a Performance-Based Design Methodology. *Fire Technology*, 53(3), pp. 1201-1232. https://doi.org/10.1007/s10694-016-0625-z

[13] British Standards Institution (1993). *BS 476-15, ISO 5660. Fire tests on building materials and structures. Method for measuring the rate of heat release of products*.

[14] Hidalgo, J.P., Torero, J.L, and Welch, S. (2018). Fire performance of charring closed-cell polymeric insulation materials: Polyisocyanurate and phenolic foam. *Fire and Materials*. https://doi.org/10.1002/fam.2501

[15] Perejón, A., Sánchez-Jiménez, P.E., Criado, J.M., and Pérez-Maqueda, L.A. (2011). Kinetic analysis of complex solid-state reactions. A new deconvolution procedure. *The journal of physical chemistry B*, 115(8), pp. 1780–91. https://doi.org/10.1021/jp110895z

[16] Fraser, R. D. B., and Suzuki, E. (1966). Resolution of Overlapping Absorption Bands by Least Squares Procedures, *Analytical Chemistry*, 38(12), pp. 1770-1773. https://doi.org/10.1021/ac60244a038

[17] Fraser, R. D. B., and Suzuki, E. (1969). Resolution of Overlapping Bands: Functions for Simulating Band Shapes, *Analytical Chemistry*, 41(1), pp. 37-39. https://doi.org/10.1021/ac60270a007

[18] Hidalgo, J.P., Welch, S., and Torero, J.L. (2015). Performance criteria for the fire safe use of thermal insulation in buildings. *Construction and Building Materials*, 100, pp. 285-297. https://doi.org/10.1016/j.conbuildmat.2015.10.014

[19] Vacca, P. (2017). Optimised fire safe and energy efficient design of insulated assemblies using a multi-criteria approach, International Master of Science in Fire Safety Engineering thesis, University of Edinburgh & The University of Queensland. [online] Available at: http://www.imfse.ugent.be/userfiles/IMFSE/files/Pascale%20Vacca%20Thesis.pdf [Accessed 1 August 2018]

[20] Hidalgo, J.P., Welch, S., and Torero, J.L. (2015). Design tool for the definition of thermal barriers for combustible insulation materials. In: *Proceedings of the 2nd IAFSS European Symposium of Fire Safety Science*. Nicosia: CERISE, p. 166.

[21] Hidalgo, J.P., Pironi, P., Hadden, R.M., and Welch, S. (2015). A framework for evaluating the thermal behaviour of carbon fibre composite materials. In: *Proceedings of the 2nd IAFSS European Symposium of Fire Safety Science*. Nicosia: CERISE, p. 195.

[22] Hidalgo, J.P., Gerasimov, N., Hadden, R.M., Torero, J.L., and Welch, S. (2016). Methodology for Estimating Pyrolysis Rates of Charring Insulation Materials using Experimental Temperature Measurements. *Journal of Building Engineering*, 8, pp. 249-259. https://doi.org/10.1016/j.jobe.2016.09.007

[23] Grayson, S. (2018) Letter to fire journal editors on materials identification in comparison of results

among fire scaling and flammability studies. https://doi.org/10.1002/fam.2642.

[24] Hidalgo, J.P. (2015) Performance-Based Methodology for the Fire Safe Use of Insulation Materials in Energy Efficient Buildings. PhD thesis, The University of Edinburgh, http://hdl.handle.net/1842/10601

[25] British Standards Institute (2004). *BS EN 520:2004. Gypsum plasterboards. Definitions, requirements and test methods*.

[26] Maluk, C., Bisby, L., Krajcovic, M., and Torero, J.L. (2016). The Heat-Transfer Rate Inducing System (H-TRIS) Test Method. *Fire Safety Journal*. https://doi.org/10.1016/j.firesaf.2016.05.001

[27] Thomas, G. (2010). Modelling thermal performance of gypsum plasterboard-lined light timber frame walls using SAFIR and TASEF. *Fire and Materials*, 34, pp. 385-406. https://doi.org/10.1002/fam.1026

[28] Keerthan, P., and Mahendran, M. (2012). Numerical studies of gypsum plasterboard panels under standard fire conditions. *Fire Safety Journal*, 53, pp. 105-119. https://doi.org/10.1016/j.firesaf.2012.06.007

[29] Ghahzi Wakili, K., Hugi, E., Wullscheleger, L., and Frank, T. (2007). Gypsum Board in Fire -- Modeling and Experimental Validation. *Journal of Fire Sciences*. 25, pp. 267-282. https://doi.org/10.1177/0734904107072883

[30] Crewe, R.J., Hidalgo, J.P., Sørensen, M.X., McLaggan, M.S., Molyneux, S., Welch, S., Jomaas, G., Torero, J.L., Stec, A.A., and Hull, T.R. (2018). Fire Performance of Sandwich panels in a Modified ISO 13784-1 Small Room Test: The Influence of Increased Fire Load for Different Insulation Materials, *Fire Technology*. 54(4), pp. 819-852. https://doi.org/10.1007/s10694-018-0703-5

[31] Zabetakis, M.G. (1965). *Flammability characteristics of combustible gases and vapours (Bulletin 627)*. [online] Washington: U.S. Dept. of the Interior, Bureau of Mines US Bureau of Mines. Available at: https://www.isa.org/pdfs/microsites121/tr-121301-reaff/ [Accessed 1 May 2016].

[32] Drysdale, D. (2011). Limits of Flammability and Premixed Flames. In: *An Introduction to Fire Dynamics*. 3rd ed. Chichester, West Sussex: John Wiley & Sons Ltd., pp. 83-119. https://doi.org/10.1002/9781119975465.ch3

[33] Drysdale, D. (1986). Fundamentals of the fire behaviour of cellular polymer. In: *Fire and Cellular Polymers*. Springer Netherlands, pp.61-75. https://doi.org/ 10.1007/978-94-009-3443-6_4

Acknowledgements

The authors would like to gratefully acknowledge funding contribution from *Rockwool International A/S* towards sponsoring the Ph.D. studies for Juan P. Hidalgo. Michal Krajcovic and Cristián Maluk are gratefully acknowledged for their lab assistance on the experimental programme.